

H₂ Production over Pt-Ni/CeO₂-SiO₂ via Ethanol Reforming in a Fluidized Bed

Vincenzo Palma, Concetta Ruocco*, Marco Martino, Antonio Ricca

Department of Industrial Engineering, University of Salerno, Via Giovanni Paolo II 132, 84084, Fisciano (SA) Italy
ruocco@unisa.it

The aim of the present work is to study the application of a fluidized bed reactor for oxidative steam reforming of ethanol (OESR) over a bimetallic 3wt% Pt-10wt% Ni/CeO₂-SiO₂ catalyst. In particular, the effect of cerium salt precursor (nitrate (N), ammonium nitrate (AN) and acetylacetonate (AC)) on catalyst activity and stability was investigated. Three catalysts were synthesized. In all cases, the support was composed of a CeO₂-SiO₂ mixed oxide and the ceria content for all the catalysts was fixed to 30 wt%. The tests were carried out at a steam to ethanol ratio (f.r.) of 4 and oxygen to ethanol ratio (o.r.) of 0.5; temperature was fixed to 500°C and the weigh hourly space velocity (WHSV) to 12.3 h⁻¹. All the samples displayed a partial deactivation with time-on-stream and ethanol was completely converted only for few hours. The initial H₂ yield was very close to the predicted thermodynamic value (41.5%) and a gradual yield lowering was observed over the three catalysts. However, after 80 h of test, all the samples reached a plateau condition, with no more variation in selectivity. It is worthwhile noting that, for the sample AC, the final conversion was attested to 75%, while the other two catalysts displayed a similar behaviour with plateau conversion of almost 60%. In addition, a higher H₂ yield (20%) was recorded after 100 h of test for the sample AC and the carbon formation rate measured after the test on the latter catalyst was almost 1 half of the values found for the catalysts N and AN: in the case of acetylacetonate, the organic group of the salt probably assures a templating effect, which protects ceria molecules, improving their dispersion and increasing catalyst activity towards both reforming and carbon gasification reactions.

1. Introduction

Nowadays, almost 96% of the global hydrogen production passes through the conversion of fossil fuels resources, thus releasing huge amount of harmful gasses in the atmosphere and leading to several environmental issues (Di Michele et al., 2019). A sustainable route for hydrogen generation having reduced effect on the global warming can be provided by the conversion of biomass-derived fuels, which are expected to assure CO₂ neutrality with respect to the greenhouse issue. For example, bioethanol is an available and efficient fuel with well-developed production and distribution infrastructures in different countries worldwide (Rodrigues S.T. et al., 2019). In addition, bioethanol is a good material for hydrogen production since it is easy to store, handle and transport, and unlike methanol, bioethanol is non-toxic.

Ethanol produced via biomass fermentation has a high water content (water/ethanol ratio of 13) and is a suitable feedstock for the reforming process (Da Costa-Serra et al., 2018). However, the ethanol steam reforming mechanism is very complex and parallel reactions (involving the formation of secondary products) can negatively affect the overall hydrogen yield; unwanted pathways responsible for carbon formation and catalyst deactivation also occur. Moreover, the steam reforming pathway is endothermic and the impact of operative costs on the global efficiency of the process can become significant. Therefore, the oxidative reforming route was proposed as an interesting alternative to overcome the typical limitation of ethanol steam reforming: the addition of proper oxygen amounts, in fact, allows auto-thermal operations and an easier gasification of coke deposits (Palma et al., 2016) compared to the steam reforming case.

The performances of the reforming process are also affected by the chosen reactor configuration. It was proved (Montero et al. 2014) that the employment of fluidized bed reactors improves the rate of heat and mass

transfer, assuring high stability during operation; a better catalytic bed uniformity with respect to the packed bed and a virtual elimination of diffusional limitations can also be reached. Moreover, under oxidative steam reforming conditions, the catalyst particles recirculation between oxidizing and reducing zones assures an easier removal of carbonaceous deposits; the level of catalyst reducibility also remain considerable, thus enhancing the reactants conversion.

Different catalytic systems have been investigated for oxidative reforming of ethanol (OESR): Ni, Co, Pt; Pd, Rh, Ir, Ru are the most common active species while Al_2O_3 , SiO_2 , CeO_2 and $\text{CeO}_2\text{-ZrO}_2$ are often selected as supports (Baruah et al., 2015). The interesting performances of a bimetallic Pt-Ni/ $\text{CeO}_2\text{-SiO}_2$ catalyst for OESR in a fluidized bed reactor, which assured very low coke selectivity, were previously described (Viviente et al., 2017). However, the dispersion of CeO_2 on the silica support can strongly affect catalyst activity and stability. Therefore, in order to investigate the latter aspect, three different ceria precursors (nitrate, ammonium nitrate and acetylacetonate) were employed for the preparation of the bimetallic catalyst and the effect of CeO_2 salt precursor on the performances of the different samples was studied.

2. Experimental

2.1 Catalyst preparation and characterization

3wt% Pt-10wt% Ni/30wt% $\text{CeO}_2\text{-SiO}_2$ catalyst from different CeO_2 precursors was prepared as follows. SiO_2 gel (90-115 μm , Sigma Aldrich) was calcined at 600°C for 3 h (heating rate of 10°C·min⁻¹) and added to the solutions of the corresponding ceria salt precursors. In the case of cerium nitrate hexahydrate and cerium ammonium nitrate tetrahydrate (supplied by Strem Chemicals), the required amount of the salt was dissolved in distilled water; then, calcined SiO_2 was added to the solution and impregnation was carried out at 80°C for two hours. Thereafter, drying at 120°C for 12 h and calcination at the same conditions reported for the SiO_2 support occurred. For the dissolution of cerium acetylacetonate hydrate (Sigma-Aldrich), a solution of 0.6/1 acetic acid/methanol (Sigma-Aldrich) was prepared and the impregnation-drying-calcination procedure was carried out as reported above. Afterwards, the sequential impregnation of active species (nickel before platinum) was carried out starting from nickel nitrate hexahydrate and platinum chloride (both provided by Strem Chemicals). The loading of metals as well as the impregnation order have been investigated in a previous work (Palma V. et al., 2015). The catalytic Pt-N/ $\text{CeO}_2\text{-SiO}_2$ samples were denoted as N, AN and AC, respectively, based on the selected salt precursor (nitrate, ammonium nitrate and acetylacetonate).

The physicochemical properties of the prepared catalysts was studied by surface area measurements (BET method), X-ray diffraction analysis (XRD) and Temperature programmed reduction (TPR) measurements.

BET surface areas were measured by nitrogen adsorption-desorption isotherms using a Sorptometer 1040 "Kelvin" by Costech Analytical Technologies. Before the measurement, samples were heated at 150°C for 1 h under vacuum.

X-ray power diffraction patterns were recorded using a D-8 Advance Bruker WAXRD diffractometer. Data were acquired over the 2 θ range of 20° to 80° and the Scherrer Equation was used to estimate the average crystallite size of CeO_2 and NiO particles.

Hydrogen temperature programmed reduction ($\text{H}_2\text{-TPR}$) of the samples was conducted in the laboratory apparatus described in Par. 2.2. The catalysts were treated by a 5% H_2/N_2 stream and heated to 700 °C at a rate of 10 °C·min⁻¹.

The spent catalysts after stability tests were characterized by means of Q600 thermo-gravimetric analyzer (TA Instrument), devoted to the estimation of carbon content. The catalysts were heated from room temperature to 1000°C (heating rate of 10°C·min⁻¹).

2.2 Laboratory Apparatus and Procedure

Oxidative steam reforming of ethanol was conducted in a fluidized bed reactor at ambient pressure. Prior to the reaction, 0.83 g of catalyst was loaded and treated under a reducing stream, as reported above. Then, the water/ethanol solution (molar ratio of ethanol to water 1:4), stored in a tank under nitrogen pressure, was fed at a rate of 26.1 g·h⁻¹ by means of a mass flow controllers for liquids (supplied by Bronkhorst High-Tech). After vaporization at 200°C, the gas mixture of H_2O , $\text{C}_2\text{H}_5\text{OH}$ and N_2 was passed through the catalytic bed; at the same time, an air stream resulting in an oxygen concentration of 5% was directly sent to the reaction section through an independent line, in order to limit the contribution of homogeneous reactions. The operative conditions were selected based on thermodynamic evaluations on the water/ethanol/nitrogen/oxygen system (Palma et al, 2016): high water to ethanol ratios improve catalyst stability by promoting the gasification reactions of the carbonaceous species eventually formed; similarly, high oxygen contents may favour the oxidation of coke, reducing, as a drawback, hydrogen production rates. Based on this observations and in order to test catalyst performances under severe conditions, the steam to ethanol ratio was fixed to 4 (slightly higher than the stoichiometric value) while an intermediate value of 0.5 was chosen for oxygen. A Weight

Hourly Space Velocity (WHSV) of $12.3 \text{ g}_{\text{ethanol}} \cdot \text{g}_{\text{catalyst}}^{-1} \cdot \text{h}^{-1}$ was selected and stability performances were evaluated at 500°C ; a quite low contact time was also chosen to test the catalyst performances under more stressful conditions. The composition of the stream exiting the reactor was quantified by a spectrophotometer (Nicolet Antaris supplied by ThermoScientific); downstream the latter analyser, the mixture was sent to a cold trap for the separation of condensable species. The hydrogen and oxygen content in the dry stream were measured by a thermal conductivity detector (Caldos 27 by ABB) and a paramagnetic instrument (Magnos 206 by ABB), respectively. Ethanol conversion ($X_{\text{C}_2\text{H}_5\text{OH}}$, (1)), hydrogen yield (Y_{H_2} , (2)), products yield (Y_i , where ν is the stoichiometric ratio between the generic product and reacting ethanol, (3)) and carbon formation rate (CFR, Eq. 4) were calculated as follows. The experimental results were compared with the equilibrium values: the thermodynamic analysis of the system $\text{H}_2\text{O}/\text{C}_2\text{H}_5\text{OH}/\text{N}_2/\text{O}_2$ was carried out by means of the software GasEq, based on the minimization of the free Gibbs energy (Skřinský J. et al., 2018).

$$X_{\text{C}_2\text{H}_5\text{OH}} = \frac{F_{\text{C}_2\text{H}_5\text{OH},\text{in}} - F_{\text{C}_2\text{H}_5\text{OH},\text{out}}}{F_{\text{C}_2\text{H}_5\text{OH},\text{in}}} \quad (1)$$

$$Y_{\text{H}_2} = \frac{F_{\text{H}_2}}{6 \cdot F_{\text{C}_2\text{H}_5\text{OH},\text{in}}} \quad (2)$$

$$Y_i = \frac{F_i}{\nu \cdot F_{\text{C}_2\text{H}_5\text{OH},\text{in}}} \quad (3)$$

$$\text{CFR} = \frac{\text{mass}_{\text{coke}}}{\text{mass}_{\text{catalyst}} \cdot \text{mass}_{\text{carbon, fed}} \cdot h} \quad (4)$$

3. Results and discussion

3.1 Catalyst characterization

As shown in Table 1, the S_{BET} of N, AN and AC sample were 217, 223 and 227 $\text{m}^2 \cdot \text{g}_{\text{cat}}^{-1}$, respectively. All the Pt-Ni/CeO₂-SiO₂ samples displayed very high specific surface areas, which is ascribable to the Pt-Ni/CeO₂ catalyst deposition on mesoporous silica gel ($400 \text{ m}^2 \cdot \text{g}^{-1}$ of surface area after calcination at 600°C for 3 hours). A good active species dispersion was also observed, with CeO₂ and NiO crystallite sizes of 6-8 nm and 9-10 nm, respectively. It is interesting to observe that the catalyst prepared from acetylacetonate assured the lowest dimension for ceria particles, which suggest that the choice of organic salt precursors can be a useful tool to improve active species dispersion.

Table 1: BET specific surface area (S_{BET}), average crystallite sizes of NiO (d_{NiO}) and CeO₂ (d_{CeO_2}), H₂ consumption from TPR.

Sample	S_{BET} ($\text{m}^2 \cdot \text{g}_{\text{cat}}^{-1}$)	d_{NiO} (nm)	d_{CeO_2} (nm)	H ₂ consumption ($\mu\text{mol}_{\text{H}_2} \cdot \text{g}_{\text{cat}}^{-1}$)
N	217	8	10	2780
AN	223	8	11	2927
AC	227	6	9	3122

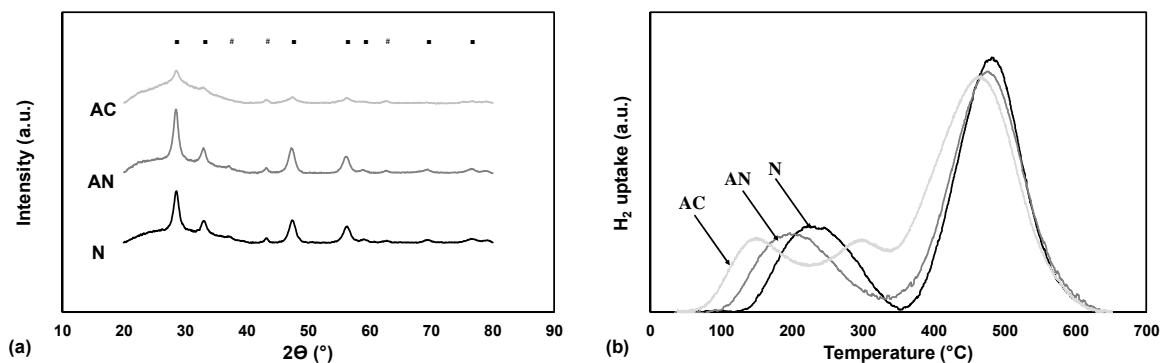


Figure 1: XRD patterns (a) and TPR profiles (b) of fresh catalysts (square: CeO₂, asterisk: NiO).

Diffraction patterns of calcined catalysts are shown in Figure 1 (a). The patterns of the catalysts N, AN and AC exhibited diffraction peaks at 2θ of 28.8° , 33.1° , 47.5° , 56.3° , 59.1° , 69.4° and 76.7° , that can be assigned to cubic CeO_2 (Hossain Tofazzel et al., 2018). In addition, the peaks of NiO can be observed at 2θ values of 37.2 and 43.2° . The absence of diffraction peaks related to platinum species implied that such species were highly dispersed on the surface of ceria supports or that their sizes were too tiny to be detected.

The XRD spectra of all the samples also have a wide hump in the range of 2θ from 20 to 40° , typical of amorphous silica phase (Feng et al., 2017). Despite the similar XRD patterns observed for the three catalysts, in the case of the AC sample, broader and less high peaks than those observed on the other two samples were detected, which proves that the employment of acetylacetonate as precursor can assure a better ceria dispersion (as also attested by the results of average crystallite sizes reported in Table 1).

H_2 -TPR profiles of the calcined catalysts are reported in Figure 1 (b). The samples prepared from nitrates (N and AN) present two reduction signals above 200 and 450°C . In the case of the catalyst prepared from the organic salt, three reduction peaks were observed, demonstrating different degrees of interaction of the support with the active species. The broad peaks observed at low temperatures are related to the reduction of PtO_x species (Franco et al., 2018). However, the interactions of platinum with nickel resulted in the formation of more reducible Ni-containing phases: the quite high H_2 uptake recorded below 400°C demonstrates that Pt presence enhances NiO reduction due to the occurrence of spillover phenomena (Palma et al., 2017): hydrogen diffuses from the just reduced metal particles towards the adjacent support, thus favouring its reduction. In fact, the addition of Pt and Ni metals promotes an earlier Ce^{4+} reduction, due to the enhanced mobility and diffusion of bulk oxygen (Palma et al., 2018a). As a result, the total consumption is considerably higher than the theoretical one ($2015 \mu\text{mol}_{\text{H}_2} \cdot \text{g}_{\text{cat}}^{-1}$), calculated based on Ni as well as Pt loadings. However, the experimental uptake increases in the order $\text{AC} > \text{AN} > \text{N}$: the choice of cerium acetylacetonate, in fact, assured the highest reducibility to the final formulation (with an experimental uptake of $3122 \mu\text{mol}_{\text{H}_2} \cdot \text{g}_{\text{cat}}^{-1}$), which is expected to enhance both catalyst activity and stability.

3.2 Catalysts performances for oxidative steam reforming of ethanol

The endurance performances of Pt-Ni/ CeO_2 - SiO_2 catalysts prepared from different ceria salt precursors were investigated at 500°C under a steam to ethanol ratio (S/E) of 4 and oxygen to ethanol ratio (O/E) of 0.5. The results are compared in Figure 2 in terms of ethanol conversion (a) and hydrogen yield (b) as a function of time-on-stream. The stability test was performed for almost 100 h in the three cases.

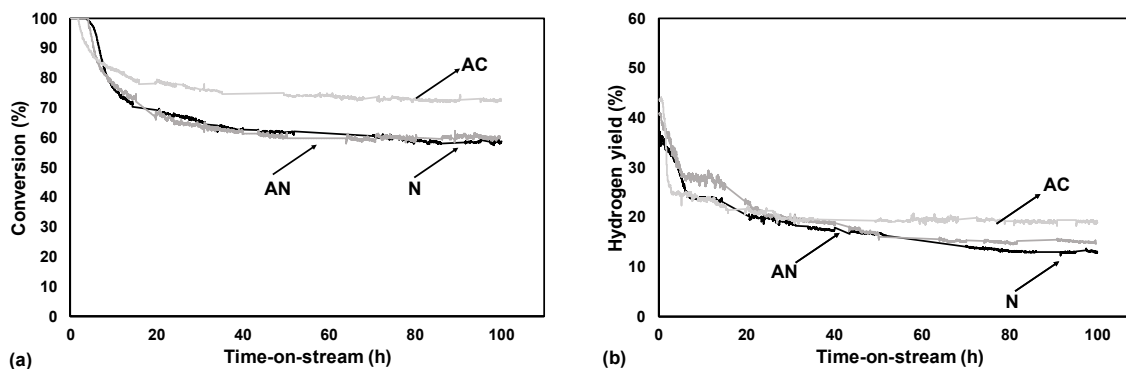


Figure 2: Ethanol conversion (a) and H_2 yield (b) during OESR stability tests over the Pt-Ni/ CeO_2 - SiO_2 catalysts; 500°C , $S/E=4$, $O/E=0.5$, $WHSV=12.3 \text{ h}^{-1}$.

Due to the quite severe operative conditions selected (the fixed contact time was of almost 150 ms and the feeding conditions only slightly higher than the stoichiometric ones), all the tested catalysts displayed initial complete ethanol conversion only for at least two hours. In addition, the initial hydrogen yield was very close to the values predicted by thermodynamic equilibrium (41.5%). However, for the Pt-Ni/ CeO_2 - SiO_2 catalysts, whatever the selected ceria salt precursor, a partial catalyst deactivation with time-on-stream was observed. For example, after almost 20 hours, ethanol conversion over the samples N and AN was of almost 70% while hydrogen yield dropped below 20%. Despite the partial activity loss observed in Figure 2, after almost 80 hours of test, both $X_{\text{C}_2\text{H}_5\text{OH}}$ and Y_{H_2} profiles approached new plateau conditions, with no more variation in product gas distribution. This behaviour, previously discussed, was explained considering that, after certain hours of test, no more accumulation of carbonaceous deposits occurred, with carbon formation and

gasification rates reaching the same value and leading to a net rate of coke accumulation equal to zero (Palma V. et al., 2018b).

The performances recorded under plateau conditions were very close for the samples prepared by nitrate and ammonium nitrate, which displayed ethanol conversion of almost 60% after 100 hours of test, with hydrogen yield quite below 20%. Conversely, the Pt-Ni/CeO₂-SiO₂ catalyst prepared starting from the organic salt displayed higher activity for oxidative steam reforming of ethanol, with $X_{C_2H_5OH}$ and Y_{H_2} attesting to 70% and 20%, respectively, at the end of the test.

A comparison was also provided between the products yield at the beginning of the test and under plateau conditions (Table 2). In the first two hours of the tests, total ethanol conversion was recorded for all the investigated samples, with a hydrogen yield higher than 34 %. In addition, acetaldehyde was not detected among the products. However, during the time-on-stream test, a change in products selectivity was observed: lower methane yield was recorded while acetaldehyde formation started being quite pronounced, especially for the samples N and AN. In contrast, the catalyst prepared from acetylacetonate, besides displaying the highest ethanol conversion and hydrogen yield, also assured reduced selectivity to by-products (i.e. C₂H₄O and coke).

Table 2: Products yield at the beginning of the test as well as under plateau conditions recorded during the experiments reported in Figure 2.

Sample	X (%)	Y _{H₂} (%)	Y _{CH₄} (%)	Y _{CO} (%)	Y _{CO₂} (%)	Y _{C₂H₄O} (%)
Products yield at the beginning of the test (mean values in the first 2 h)						
N	100	34.2	33.1	12.3	50.9	-
AN	100	34.4	32.7	11.9	51.7	-
AC	100	35.3	31.2	12.6	53.1	-
Products yield at the end of the test (mean values in the last 20 h)						
N	59.3	13.1	10.9	25.6	5.6	18.9
AN	60.1	15.4	5.5	31.5	4.5	18.1
AC	73.3	19.4	12.2	30.1	19.1	11.1

In this regard, after stability measurements, the three samples were characterized by specific area measurements as well as thermo-gravimetric analysis; S_{BET} as well as CFR, estimated according to Eq.4, are reported in Table 3. For all the tested samples, a surface area reduction was observed, ascribable to the occlusion of catalysts meso-pores by carbonaceous deposits. Conversely, the sample prepared from cerium acetylacetonate underwent a variation of specific surface area of only 9 % and the recorded value of carbon formation rate was almost 1 half that measured over the catalysts synthesized from nitrates.

Table 3: Carbon formation rates measured after the stability tests in Figure 3.

Sample	S_{BET} (m ² ·g ⁻¹)	Carbon Formation rates (g _{coke} ·g _{catalyst} ⁻¹ ·g _{carbon, fed} ⁻¹ ·h ⁻¹)
N	169	3·10 ⁻⁶
AN	175	2.9·10 ⁻⁶
AC	206	1.4·10 ⁻⁶

These results confirmed that the higher performances of the AC catalyst are related to its reduced coke accumulation tendency. The better activity and stability of the catalyst prepared from acetylacetonate is ascribable to the chemical structure of the salt, markedly different from that of the nitrates. During the preparation of the CeO₂-SiO₂ support, in fact, the organic group of the salt assures a templating effect, improving the dispersion of CeO₂ particles (as also attested by the results of XRD analysis reported in Table 1). In particular, the organic group of the salt is able to assure a proper stereochemical position to cerium ions, which prevents CeO₂ sintering and assures higher catalytic performances to the final catalyst compared to the samples prepared from other precursors. Also other authors (Bensalem et al., 1995) found that the employment of acetylacetonate as salt precursor for the preparation of CeO₂-SiO₂ mixed oxides leads to lower dimensions of ceria particles compared to nitrates. As a consequence of the improved active species dispersion, the catalyst AC displayed better activity towards both reforming and carbon gasification reactions with respect to the N as well as AN samples.

4. Conclusions

In the present work, oxidative steam reforming of ethanol has been investigated over Pt-Ni/CeO₂-SiO₂ catalysts prepared by wet impregnation from different ceria salt precursors (nitrate, ammonium nitrate, acetylacetonate). The activity and stability of the samples was studied at 500°C under a H₂O/C₂H₅OH ratio of 4 and O₂/C₂H₅OH ratio of 0.5. A quite high space velocity was selected (WHSV=12.3 h⁻¹) in order to evaluate the catalyst behaviour under more stressful conditions. The results of catalyst characterization revealed the good active species dispersion and the high reducibility of the sample prepared from the organic precursor. During time-on-stream tests, all the samples displayed a partial deactivation; however, after almost 80 h, a new stationary condition was recorded, corresponding to a net rate of carbon formation equal to zero. However, the catalyst prepared from acetylacetonate was attested to higher values in terms of both ethanol conversion and hydrogen yield. The results of spent catalyst characterization proved the lower extent of carbon deposition on the latter sample: the choice of acetylacetonate as salt precursor assures a templating effect, promoting ceria dispersion and improving catalyst activity towards both reforming and carbon gasification reactions.

References

- Baruah R., Dixit M., Basarkar P., Parikh D., Bhargav A., 2015, Advances in ethanol autothermal reforming, *Renewable and Sustainable Energy Reviews* 51, 1345–1353.
- Bensalem A., Bozon-Verduraz F., Delamar M., Bugli G., 1995, Preparation and characterization of highly dispersed silica-supported ceria, *Applied Catalysis A: General*, 121, 81-93.
- Da Costa-Serra J.F., Chica A., 2018, Catalysts based on Co-Birnessite and Co-Todorokite for the efficient production of hydrogen by ethanol steam reforming, *International Journal of Hydrogen Energy*, 43, 1659-65.
- Di Michele A., Dell'Angelo A., Tripoldi A., Bahadori E., Sanchez F., Dimitratos N., Rossetti I., Ramis G., 2019, Steam reforming of ethanol over Ni/MgAl₂O₄ catalysts, *International Journal of Hydrogen Energy*, 44, 952-964.
- Feng Q., Wang L., Su L., Xu S., 2017, Preparation of TiO₂@SiO₂ with a Hollow Olive-shaped Cable by Electrospinning, *Chemical Engineering Transactions*, 60 (2017) 109-114.
- Franco P., Martino M., Palma V., Scarpellini A., De Marco I., 2018, Pt on SAS-CeO₂ nanopowder as catalyst for the CO-WGS reaction, 43, 19965-19975.
- Hossain Tofazzel S.T., Azeeva E., Zhang K., Zell E.T., Bernard D.T., Balaz S., Wang R., 2018, A comparative study of CO oxidation over Cu-O-Ce solid solutions and CuO/CeO₂ nanorods catalysts, *Applied Surface Science*, 455, 132-143.
- Montero C., Valle B., Bilbao J., Gayubo A.G., 2014, Analysis of Ni/La₂O₃- α Al₂O₃ Catalyst Deactivation by Coke Deposition in the Ethanol Steam Reforming, *Chemical Engineering Transactions*, 37, 481-486.
- Palma V., Ruocco C., Ricca A., 2015, Bimetallic Pt and Ni Based Foam Catalysts for Low-Temperature Ethanol Steam Reforming Intensification, 43, 559-564.
- Palma V., Ruocco C., Meloni E., Ricca A., 2016, Activity and stability of novel silica-based catalysts for hydrogen production via oxidative steam reforming of ethanol, *Chemical Engineering Transactions*, 52, 67-72.
- Palma V., Ruocco C., Meloni E., Ricca A., 2017, 166, Highly active and stable Pt-Ni/CeO₂-SiO₂ catalysts for ethanol reforming, *Journal of Cleaner Production*, 166, 263-272.
- Palma V., Martino M., 2018a, Aluminum Foam based Catalysts for the CO-WGS Reaction, *Chemical Engineering Transactions*, 70, 1225-1230.
- Palma V., Ruocco C., Ricca A., 2018b, Oxidative steam reforming of ethanol in a fluidized bed over CeO₂-SiO₂ supported catalysts: effect of catalytic formulation, *Renewable energy*, 125, 356-364.
- Rodrigues S.T., de Moura A., Silva F., Candido E., da Silva A., de Oliveira D., Quiroz J., Camargo P., Bergamaschi V., Ferreira J., Linardi M., Fonseca F., 2019, Ni supported Ce_{0.9}Sm_{0.1}O_{2- δ} nanowires: An efficient catalyst for ethanol steam reforming for hydrogen production, *Fuel*, 237, 1244-53.
- Skřínský J., Ochodek T., 2018, Influence of Initial Temperature on Explosion Severity Parameters of Methanol/Air Hybrid Mixture Measured in 1-m³ Vessel, *Chemical Engineering Transactions*, 67, 175-180.
- Viviente, J.L., Meléndez, J., Pacheco Tanaka D.A, Gallucci, F., Spallina, V., Manzolini, G., Foresti, S., Palma V., Ruocco, C., Roses, L., 2017, Advanced m-CHP fuel cell system based on a novel bio-ethanol fluidized bed membrane reformer, *International Journal of Hydrogen Energy*, 42, 13970-13987.